IEEE Access
Multidisciplinary | Rapid Review | Open Access Journal

Received December 11, 2020, accepted December 12, 2020, date of publication December 16, 2020,
date of current version December 30, 2020.

*Digital Object Identifier 10.1109/ACCESS.2020.3045287*

# A Zero Placement Algorithm for Synthesis of Flat Top Beam Pattern With Low Sidelobe Level

**SHAOWEI DAI, MINGHUI LI, (Member, IEEE), QAMMER H. ABBASI, (Senior Member, IEEE), AND MUHAMMAD ALI IMRAN, (Senior Member, IEEE)**
School of Engineering, University of Glasgow, Glasgow G12 8QQ, U.K.
Corresponding author: Shaowei Dai (s.dai.2@research.gla.ac.uk)

This work was supported by the Singapore Economic Development Board and Singapore RFNet Technologies Pte. Ltd.

**ABSTRACT** Flat top beam pattern synthesis is increasingly important for beamformer in high mobility scenarios due to the rapid change of Direction of Arrival (DOA). A Zero Placement for Flat Top (ZPFT) beam pattern synthesis algorithm is presented in this article. It works in Z domain directly and breaks down the total response into two portions. The first portion satisfies the beamwidth requirement with low Sidelobe Level (SLL) which is realized through algorithms like Dolph-Chebyshev algorithm. The second portion is then used to create a broadening effect. The location of the broadening zeros are derived using principles result from the broadening effect analysis of two quadratic functions. Compared to conventional Finite Impulse Response (FIR) method or iterative methods, the proposed method identifies the zeros of the array factor directly and computes the weight without iteration. Since it works in the spatial angle domain directly, the steering of the mainlobe beam could be implemented through a simple angle shift. Numerical simulation confirms the effectiveness of the algorithm. ZPFT can achieve 22dB lower SLL while maintaining the same main beam performance as compared with FIR method for an Uniform Linear Array (ULA) with **7** elements. It can achieve the same optimal performance as the iteration based global optimisation techniques like Semi-Definite Relaxation (SDR) with about 380 times less computing time in an Intel Core i7 Windows platform. ZPFT can steer the main beam easily in real time. All these make it an ideal candidate for high mobility applications where the DOA changes rapidly.

**INDEX TERMS** Beamforming, flat top, synthesis, high mobility.

## I. INTRODUCTION

Beamforming is widely used in wireless communication as a spatial filter to enhance signals from a specific Direction of Arrival (DOA) and suppress noise and interference from other directions. In high mobility scenarios, wireless communication with beamforming faces unique challenge [1] where the DOA changes rapidly which makes the beamforming performance degrade or fail if not addressed properly. It is always desirable to tune the beamwidth of the mainlobe to cater for the mismatch of DOA due to estimation error or inaccuracy of element calibration. Various robust algorithms [2]–[4] have been proposed to cater for the mismatch of DOA by putting in constraints to broaden the main beam. The Flat Top shaped beam pattern [5]–[9] is thus increasingly attractive due to its flat response to large DOA mismatch especially in high mobility scenario when the DOA changes more rapidly.

Beam pattern synthesis is an extensively investigated area in antenna array beamforming design. Many algorithms have been proposed in the literature to achieve the optimization of low Sidelobe Level (SLL) [10], [11], high gain and narrow mainlobe. Schelkenoff [12] established the link between nulls of the beam pattern and the complex roots of the polynomials that represent the $Z$ transform of the beamformer weights. By spacing out the zeros in the unit circle differently, many patterns could be synthesized. Dolph [13] proposed to use the properties of Chebyshev polynomials [14] of the first kind to achieve equal Sidelobe Level and the narrowest main beam. Subsequently, Riblet [15] discovers that Dolph's method only applies to scenarios where the antenna elements spaced at least half wavelength.

The associate editor coordinating the review of this manuscript and approving it for publication was Giorgio Montisci.

The original Dolph-Chebyshev array is then extended to scenarios with less than half wavelength inter-element space where a different mapping could be applied to use the Chebyshev polynomials. A similar pattern for continuous apertures is proposed by Taylor [16] with a modification that the far out of the sidelobes can decay faster following a uniform array pattern while keeping the sidelobes close to the mainlobe with equip-ripple as in Dolph-Chebyshev array. To implement the same pattern directly for a discrete array, Villeneuve [17] proposed a method to replace the last few zeros of the array response with the zeros of a uniform array. Different window methods like Gaussian [18] and the derivative of Chebyshev [19] have been reported to get a decaying sidelobe shape with narrower main lobe for improved efficiency. In [20], a modified Chebyshev array is proposed to make the SLL, beamwidth to be adjustable independently. But since the modified function is non-linear and can't be expressed as polynomials, an iterative method has to be used to derive the converged weight.

Although these methods synthesize beam patterns with low SLL, narrow or adjustable main beam, the shaped beam pattern is not part of their optimization goal. To get flat-top beam pattern, Finite Impulse Response (FIR) based algorithms and various numerical optimization algorithms over an objective or cost function could be used. Window method [5] based on FIR algorithm is popular due to its robustness and easy for implementation. But due to its extra constraints of the same level of ripples in pass band and stop band, it is not optimum for the filter order [21]. Iterative methods based on numerical optimization algorithms like minimum mean squared optimization [22], or stochastic based Genetic Evolution algorithm [23], Particle Swarm Optimization algorithm [6], [24] and various convex optimization based algorithms [25] normally are used for getting shaped main beam. However iterative methods might not be suitable for high mobility scenarios where real-time calculation usually is needed.

In this article, the Zero Placement method based on Schellkenoff polynomial is used to synthesize Flat Top beam pattern directly. Although a similar concept of zero replacement is used in [17], their adjustment is still restricted on the unit circle. So its effect in the main beam is limited to the null-to-null beamwidth and gain. And the main beam shape can not be controlled. In this article, by relaxing this restriction, the zeros can be placed off the unit circle instead of replacing part of the Dolph-Chebyshev zeros with uniform array zeros located on the unit circle. This step makes the main beam shape controlling possible. The proposed ZPFT algorithm breaks the array factor into two parts. For an $N$ elements antenna array which has $N-1$ zeros of freedom for beam pattern control, two of the zeros are reserved for synthesizing the flat-top shaped main beam. The rest $N-3$ zeros can be used for any other existing low SLL window methods. Due to the unique feature that forms narrowest mainlobe with a given Sidelobe Level (SLL) or lowerest SLL with a given null to null beamwidth of mainlobe, Dolph-Chebyshev array is chosen for the $N-3$ zeros allocation. But other window functions could also be used. The key innovation for this article is two folds. Firstly, the off unit circle zeros are explored directly to mix with unit circle zeros from Dolph-Chebyshev to control the main beam shape. Secondly, the quadratic function approximation is used to investigate the flat-top effect of the proposed zero location and an algorithm is developed to identify the location of zeros for flat-top control. So that it achieves lower SLL compared with FIR method with the same flat-top pattern directly with simple zero placement in the spatial angle domain. This also makes the steering of the main beam straightforward. Further more, when comparing to iteration based global optimization methods, it achieves the same optimum beam pattern and takes 380 times less computing time in an Intel Core i7 Windows platform as the simulation shows for an ULA with 8 elements. All these make ZPFT an ideal candidate for high mobility applications where the DOA changes rapidly. To the best of our knowledge, it is the first time Dolph-Chebyshev zeros are combined with the off unit circle zeros to realize flat-top main beam shape while preserving the narrow main beam property. This different way of zero arrangement makes ZPFT simple yet effective and gives ZPFT the advantage of synthesizing flat-top shaped beam patterns while maintaining low SLL in a steering adjustment efficient way compared with existing methods in the literature.

The article is organized as follows, after the problem model is established in section II, the zero placement algorithm for synthesizing flat-top beam pattern is described in section III. Numerical simulation is conducted in section IV which compares the proposed algorithm with the existing algorithms. In the end section V concludes the article.

## II. PROBLEM FORMULATION

For clarity of the discussion, a system model for Uniform Linear Array (ULA) with $N$ antenna elements is illustrated in Fig. 1.

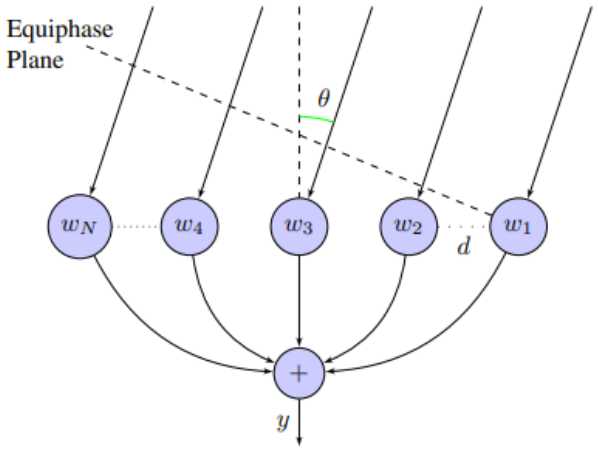


**FIGURE 1.** Beamformer model of received signal.

The received signal $x_i(t)$ on the $i^{th}$ element from a signal $s_\theta(t)$ incident from an angle $\theta$ could be expressed as

$$\begin{aligned} x_i(t) &= s_\theta(t)e^{-j\frac{2\pi dsin(\theta)}{\lambda}(i-1)} \\ &= s_\theta(t)e^{-j2\pi(i-1)\xi} \end{aligned} \tag{1}$$

where $\lambda$ indicates the wavelength, and $\xi = 2\pi\frac{dsin(\theta)}{\lambda}$ is the spatial frequency.

The beamformer output $y(t)$ in this narrow band model could then be expressed as [26, p. 4]

$$\begin{aligned} y(t) &= \sum_{i=1}^{N} w_i x_i(t) \\ &= s_\theta(t)\sum_{i=1}^{N} w_i e^{-j(i-1)\xi} \end{aligned} \tag{2}$$

So the spatial frequency response could be defined as

$$H(\xi) = \sum_{i=1}^{N} w_i e^{-j(i-1)\xi} \tag{3}$$

It could also be written in the $Z$ transform format [27, p. 109] as

$$H(z) = \sum_{i=1}^{N} w_i z^{-(i-1)} \tag{4}$$

According to Schelkunoff [12], every ULA could be represented as a polynomial and vice versa. According to fundamentals of polynomial, the Array Factor (AF) defined by (4) could be factored by its (N-1) roots as

$$\|H(z)\| = \left\|\prod_{i=1}^{N-1}(z - z_i)\right\| \tag{5}$$

where each $z_i$ gives a null response for the angle that defined by $e^{j\xi_i} = z_i$ and $z = e^{j\xi}$ is evaluated along the unit circle. As indicated in (5), the Array Factor for a $N$ elements array could be uniquely characterized by its $N-1$ zeros.

So the objective of this article is to synthesize a flat-top beam pattern with low SLL by identifying the proper location of zeros.

## III. PROPOSED SOLUTION

For ULA, the number of zeros uniquely defines the $Z$ transform of the weight vector thus also defines the array factor. Inspired by the concept of [1], the polynomial of $Z$ (4) could break into two parts.

$$H(z) = C(z)B(z) \tag{6}$$

where $C(z)$ corresponds to the sub-polynomial that generates beam pattern without flattening constraints, and $B(z)$ represents the portion that compensates and flattens the main lobe. $N-3$ zeros are allocated for $C(z)$ as

$$C(z) = \prod_{i=3}^{N-1}(z - z_i) \tag{7}$$

which represents the sub-array that controls the main beam width and SLL. Two zeros are allocated for $B(z)$ as

$$B(z) = (z - z_1)(z - z_2) \tag{8}$$

which represents the broadening sub-array that creates the flat-top and decaying far-out sidelobes.

### A. NARROW MAINLOBE BEAM WIDTH WITH LOW SLL CONTROLLED BY C(z)

In this article, the sub-array represented by $C(z)$ is implemented through the Dolph-Chebyshev algorithm due to its simplification. For clarity, the inter element space is assumed to be half wavelength. Since two zeros represented by $B(z)$ are reserved for the flat-top control, the actual elements for implementing the Dolph-Chebyshev array will be $N-2$ elements.

In Dolph-Chebyshev array, there is only one scaling parameter $R_0$ that controls both the main beam width and SLL which maps the spatial frequency $\xi$ range to the abscissa of the Chebyshev polynomial range [15]. The Chebyshev polynomial used for $C(z)$ could be defined as

$$T_{N-3}(x) = \begin{cases} \cos((N-3)\cdot\arccos(x)), & \text{for } |x| \le 1 \\ \cosh((N-3)\cdot acosh(x)), & \text{for } |x| > 1 \end{cases} \tag{9}$$

where $x = R_0\cos(\frac{\xi}{2})$ is the scaled input for the Chebyshev polynomial. The scaling factor $R_0$ could be derived from the null to null beam width as:

$$R_0 = \cos(\frac{\pi}{2(N-3)})\cdot 1/\cos(\pi\frac{d}{\lambda}\cdot\sin(bw/2)) \tag{10}$$

where $bw$ is the required null to null beam width.

By setting $T_{N-3}(x) = 0$ for $|x| \le 1$, all the $N-3$ zeros could be found as [28, p. 1147]

$$\xi_i = 2\cdot\arccos(\frac{x_i}{R_0}) \tag{11}$$

where $x_i = \cos\frac{(i-1/2)\pi}{N-3}$, $i = 1, 2, \ldots, N-3$.

### B. ZERO PLACEMENT FOR FLAT TOP CONSTRAINTS SUB-ARRAY B(z)

To find the zero locations of $B(z)$ to flatten the beam pattern of the main lobe, it would be necessary to understand the pattern around the main lobe and the impact of the location of zero $(r_0, 0)$ on the pattern.

As illustrated in Fig. 2, each angle $\xi = \frac{2\pi d}{\lambda}\sin(\theta)$ corresponds to a DOA $\theta$. The main lobe is assumed at point $c$ which corresponds to 0 degree measured from the broadside. It is clear from Fig. 2 that $|z - r_0|$ reaches the minimum when $z$ is at $c$ which corresponds to the main lobe.

The distance $d_{r_0}$ between $z$ and $r_0$ could be described as (12).

$$\begin{aligned} d_{r_0}(\xi) &= |z - r_0| \\ &= \sqrt{1 - 2\cos(\xi)r_0 + r_0^2} \end{aligned} \tag{12}$$

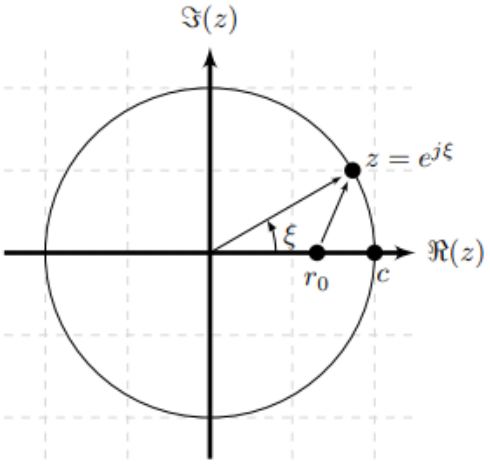


**FIGURE 2.** Norm $|z - r_0|$ for a zero placed at $(r_0,0)$ .

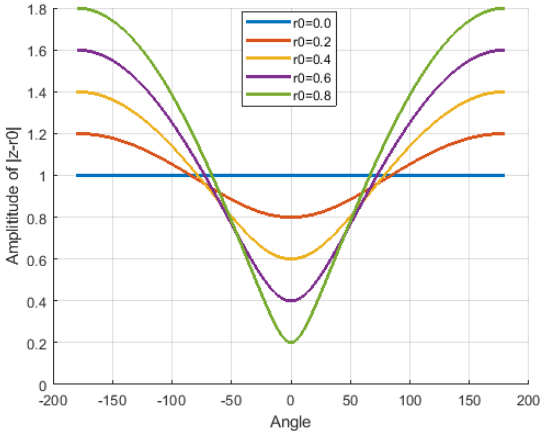


**FIGURE 3.** Zero location effect on amplitude response.

To further investigate the curve effect of $r_0$, $d_{r_0}(\xi)$ could be expanded using the second order Taylor series around point $c$ which corresponds to the main lobe at $\xi = 0$ as

$$d_{r_0}(\xi) \approx \hat{d_{r_0}} = d_{r_0}(0) + d'_{r_0}(0)\xi + \frac{1}{2}d''_{r_0}(0)\xi^2 \tag{13}$$

where $d'_{r_0}$,$d''_{r_0}$ indicates the first and second derivative of $d_{r_0}$ respectively. After taking derivative of (12 ), it is easy to find out that:

$$d'_{r_0}(0) = \left.\frac{r_0 \sin(\xi)}{\sqrt{1 - 2\cos(\xi)r_0 + r_0^2}}\right|_{\xi=0} = 0 \tag{14}$$

$$d''_{r_0}(0) = d''_{r_0}(\xi)\big|_{\xi=0} = \frac{r_0}{1 - r_0} \tag{15}$$

So the second order Taylor series could be expressed:

$$\hat{d}_{r_0}(\xi) = \frac{r_0}{2(1 - r_0)}\xi^2 + 1 - r_0 \tag{16}$$

For using this as a broadening function, the shaping parameter is derived as

$$\begin{aligned} k_b &= \frac{d_{r_0}}{\frac{1}{2}d''_{r_0}} \\ &= \frac{2(1 - r_0)^2}{r_0} \end{aligned} \tag{17}$$

Fig. 3 shows the effect of zero location on the amplitude response. It is clear that when $r_0$ moves to the origin, it gives an all-pass response that will not change the amplitude response. On the other hand, when $r_0$ moves towards the unit circle, it creates a dip at the main lobe.

By examining the effect of zeros in Fig. 3, the dip effect at angle 0 could be used for creating the flat-top pattern in the mainlobe. So the $z_1$ could be just located in the real axis and off the unit circle at $(r_0, 0)$. Fig. 3 shows that the broadening zero at $z_0$ has a side effect of raising the far-out sidelobe level as also indicated in [29]. An extra zero (-1,0) could then put in to compensate for the effect. So the two zeros for $B(z)$ could be designed as:

$$B(z) = (z - r_0)(z + 1) \tag{18}$$

With (6),(9),(18), the transfer function could be derived as:

$$H(z) = T_{N-3}(R_0 \cos(\pi \frac{d}{\lambda} \sin(\theta)))(z - r_0)(z + 1) \tag{19}$$

where $\theta$ is the azimuth angle. The power distribution of the beam pattern could then be evaluated along the unit circle as:

$$P(\theta) = |T_{N-3}(R_0 \cos(\frac{\pi d}{\lambda} \sin(\theta))(z - r_0)(z + 1)|^2_{z=e^{j\frac{2\pi d}{\lambda}\sin(\theta)}} \tag{20}$$

### C. PRINCIPLE CONDITION FOR FLATTENING A SECOND ORDER POLYNOMIAL WITH A BROADENING POLYNOMIAL

The flat-top effect of the zero $z_0$ is investigated through an approximation with a second order polynomials in this section. For a second order even polynomial that have a curvature peak at $x = 0$,

$$f(x) = -a_1x^2 + b_1 \tag{21}$$

where $a_1 > 0$ and $b_1$ can be any real value, a broadening polynomial

$$b(x) = a_2x^2 + b_2 \tag{22}$$

where $a_2 > 0$ could be applied to obtain a flat-top function

$$p(x) = f(x)b(x) \tag{23}$$

where $p(x)$ represents a resultant function that has a flat-top. To get the condition for broadening function $b(x)$ to be effective, the derivative of (23) could be investigated

$$\begin{aligned} p'(x) &= \frac{d}{dx}(-a_1x^2 + b_1)(a_2x^2 + b_2) \\ &= x(-4a_1a_2x^2 + 2(-a_1b_2 + a_2b_1)) \end{aligned} \tag{24}$$

where $\frac{d}{dx}$ indicates the derivative operator.

By forcing (24) to 0, the peak of $p(x)$ could be located as

$$x_0 = 0 \tag{25}$$

$$x_{1,2}^2 = \frac{1}{2}\left(\frac{b_1}{a_1} - \frac{b_2}{a_2}\right) \tag{26}$$

where $x_0$ represents the original peak location, $x_{1,2}$ is the two possible peak locations introduced by the broadening polynomial.

By defining shape parameters as

$$k_f = \frac{b_1}{a_1} \tag{27}$$

$$k_b = \frac{b_2}{a_2} \tag{28}$$

and controlling factor as

$$k = \frac{k_b}{k_f} \tag{29}$$

where $k_f$, $k_b$ is the shape parameter for original function and broadening function respectively, and $k$ is the controlling factor for regulating the broadening effect, (26) could be simplified as:

$$x_{1,2}^2 = \frac{1-k}{2} k_f \tag{30}$$

In the practical beamforming context, $k_f > 0$ is always satisfied. With this assumption, the principle condition for the broadening polynomial could be summarized as:

$$p(x) = \begin{cases} \text{no flat top,} & \text{for } k > 1 \\ \text{flat top,} & \text{for } k = 1 \\ \text{flat top with variation,} & \text{for } k < 1 \end{cases} \tag{31}$$

This concept is illustrated with an example polynomial $f_1(x) = 2x^2 + 20$ in Fig. 4. It shows that with $k = 1$, the production patched function $p(x)$ has a flat-top without variation. When $k = 0.2, 0.5, 0.7$, the top is broadened but also exhibit a dip in the original top. The smaller the $k$ value, the deeper the dip and the wider the broadening effect. As a contrast, it barely shows the broadening effect when $k = 3$. It could be explained from (26), when $k > 1$, there is no real roots for (24) except at $x = 0$ which means there is only one extreme point: the original top point.

Since the peak occurs at the extreme point $x_1$, $x_2$ and the dip occurs at $x_0$, the variation within the broadened range could be easily calculated as:

$$\delta = \frac{p(x_1)}{p(x_0)} = \frac{(1+k)^2}{4k} \tag{32}$$

where the $\delta$ represents the variation within the broadened band and $k$ is the controlling factor as defined in (26).

So for a given $\delta$, the controlling factor $k$ could be derived as

$$k = 2(\delta - \sqrt{\delta^2 - \delta}) - 1 \tag{33}$$

by finding the roots of (32).

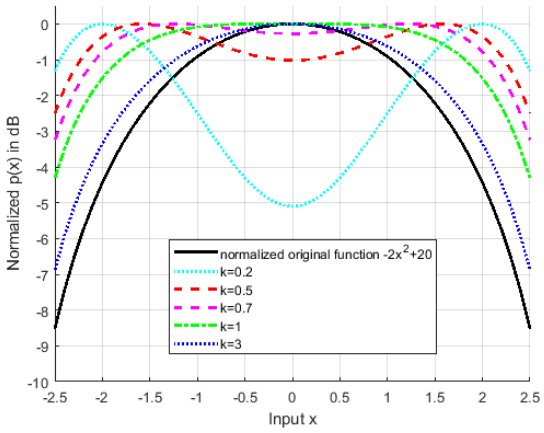


**FIGURE 4.** Concept to flatten a second order even polynomial function.

### D. MAIN LOBE PATTERN APPROXIMATION BY TAYLOR SERIES EXPANSION

In the main lobe region, the beam pattern could be Taylor expanded to get a second order polynomial approximation as

$$f(\xi) = \cosh(Nx) \approx f(\hat{\xi}) = f(0) + f'(0)\xi + \frac{1}{2}f''(0)\xi^2 \tag{34}$$

where $x = acos(R_0 cos(\xi))$ represents the normalized angle, and $f'(\cdot), f''(\cdot)$ indicates the first and second derivative operator of $f(x)$ respectively. With simple manipulation, the the derivatives could be derived as:

$$f'(0) = N \cdot \sinh(Nx) \frac{(-R_0 \sin(\xi))}{\sqrt{R_0^2 \cos(\xi)^2 - 1}}\bigg|_{\xi=0} = 0 \tag{35}$$

$$f''(0) = f''(\xi)\big|_{\xi=0} = N \cdot \sinh(Nx) \frac{-R_0}{\sqrt{R_0^2 - 1}} \tag{36}$$

Treat this expansion as the original function to be broadened, the shape parameter could be derived as

$$k_f = \frac{f(0)}{-\frac{1}{2}f''(0)} = \frac{2\sqrt{R_0^2 - 1}}{R_0 N \cdot \tanh(Nx)} \approx \frac{2\sqrt{R_0^2 - 1}}{R_0 N} \tag{37}$$

where the approximation is made due to $\tanh(Nx)|_{\xi=0} \approx 1$. The location of $r_0$ for the broadening could then be derived according to (29) as

$$\frac{(1-r_0)^2}{r_0} = \frac{k\sqrt{R_0^2 - 1}}{N \cdot R_0} \tag{38}$$

Solving (38), $r_0$ could be derived as:

$$r_0 = 1 + \frac{1}{4}\left(kk_f \pm \sqrt{(kk_f)^2 + 8kk_f}\right) \tag{39}$$

where $k$ is the controlling factor as defined in (29) and $k_f$ is the original function to be broadened as defined in (37). One interesting finding from (39) is that there are two $r_0$ satisfy the requirement. They are conjugated to each other in the complex angle sense [30]. For beamforming implementation purpose, the $r_0 < 1$ will be taken.

### E. ALGORITHMS FOR THE SYNTHESIS OF FLAT TOP BEAM PATTERN

With the preparation of the previous sub-section, the algorithm for the synthesis of flat-top beam pattern could then be described as a 3 steps process. Firstly, based on the input requirement of number of antenna elements $N$ and SLL value or Beamwidth, the $N-3$ zeros of the $N-2$ elements Chebyshev array are calculated. Secondly, based on the requirement of the allowed variation, the last two zeros location are calculated. In the end, the complete $N$ weights are derived from the whole $N-1$ zeros. The details of the algorithm are described below.

**Algorithm 1** Synthesis of Zero Placement Controlled Flat Top Beam Pattern

**Require:** Input($N$, $sll$, $bw$, $d$, $\lambda$,$\delta$)
$N$: Number of Antenna Elements
$sll$: Sidelobe Level
$bw$: Null to Null Mainlobe Beamwidth
$d$: Antenna Element Space
$\lambda$: Wave Length of Incident Signal
$\delta$: Allowed Variation in the mainlobe beam

1: //Derive $R_0$ for $(N-2)$ elements based on $sll$ or $bw$
2: **if** $sll! = null$ **then**
3: $L = 10^{sll/20}$
4: $R_0 = \cosh(\frac{acosh(L)}{(N-3)})$;
5: **else**
6: $R_0 = cos(\frac{\pi}{2(N-3)}) \cdot 1/cos(\pi \frac{d}{\lambda} \cdot \sin(\frac{bw}{2}))$
7: **end if**
8: //Find all zeros for Chebyshev sub-polynomial
9: **for** $i$ in 1 to $(N-3)$ **do**
10: $z_{i+2} \Leftarrow e^{j \cdot 2 \cdot acos(\frac{1}{R_0} cos(\frac{(2i-1)\pi}{2(N-3)}))}$
11: **end for**
12: //Find a proper controlling factor $k$ based on allowed variation $\delta$
13: $k = 2(\delta - \sqrt{\delta^2 - \delta}) - 1$
14: //Derive shape parameter $k_f$ for the second order Taylor expansion of Chebyshev Response
15: $k_f = \frac{2\sqrt{R0^2-1}}{R_0(N-3)}$
16: //Derive $r_0$ for the broadening zero location
17: $r_0 = (1 + \frac{1}{4}(kk_f \pm \sqrt{(kk_f)^2 + 8kk_f})) \cdot \alpha$
18: $z_1 \Leftarrow r_0$
19: $z_2 \Leftarrow -1$
20: $C(z) \Leftarrow \prod_{i=1}^{N-1}(1 - z_i z^{-1})$
21: **for** i in 0 to N-1 **do**
22: $w(i+1) \Leftarrow$ coefficient of $z^{-i}$
23: **end for**

For a $N$ element Uniform Linear Array (ULA), there are total $N-1$ zeros for distribution. In steps 1 to 11, $N-3$ zero are used to build the Chebyshev array using the SLL or Beamwidth constraints. The left two zeros are used for the broadening effect. In steps 12-13, the controlling factor is decided, there is some flexibility for the value of $k$ and it depends on how much variation is allowed inside the main beam. In steps 14-15, the second order Taylor expansion is used to approximate the Chebyshev response, so that the broadening theory developed using the second order polynomial could be used to calculate the shape parameter $k_f$. Then in steps 17-18, the location of the broadening zero $r_0$ is derived. During implementation, an optional adjustable factor $\alpha$ could be applied to $r_0$ to compensate for the approximation error. In practice, $\alpha = 0.9$ gives a good matching result. In step 19, an extra zero is placed at (-1,0) to balance the effect of $r_0$ for remaining low SLL.

## IV. NUMERICAL SIMULATION AND ANALYSIS

To verify the performance of the proposed ZPFT algorithm, two simulations are set up for the comparison with two type of popular algorithms, window method and numerical optimization method. The third simulation is to show the ripple effect of the $k$ factor and the easy steering of the flat-top main beam. The window method based on FIR algorithm is popular due to its simplicity although not optimum [21] as it just applies a window function to an ideal filter response to smooth out the transition band. Recently, the convex optimization for beam pattern synthesis becomes more and more popular with the readily available optimization packages like CVX [31]. When shaped beam pattern synthesis is formulated as an optimization problem, the constraints on the amplitude in the pass band is often non-convex. One of the most promising way to apply convex optimization is to use the Semi-definite Relaxation (SDR) algorithm which drops the rank one requirement of the correlation matrix to make it a convex optimization program [32]–[34].

### A. LOWER SLL OR NARROWER NULL TO NULL BEAMWIDTH COMPARED WITH WINDOW METHOD

In the first simulation, ZPFT is compared with window method based on FIR and Dolph-Chebyshev to demonstrate that ZPFT is able to deliver the same main beam as the window methods but with much lower SLL or narrower null to null beamwidth. A 7 elements ULA with flat-top beam pattern with -52dB SLL as designed in [5] is used for comparison for FIR based algorithm. The design parameter is listed below in Table (1).

Fig. 5 shows the performance of the synthesized beam pattern following the requirements in Table (1). ZPFT algorithm can be controlled by beamwidth or SLL. Both methods are used in this simulation for comparison. It shows clearly that while FIR algorithm used in [5] does make a flat-top beam pattern, the synthesized SLL is around -52.7dB. In contrast, the proposed ZPFT algorithm by beamwidth gives a much lower SLL of around -75dB with the same broadened flat-top

**TABLE 1. Design Parameter for Simulation of Comparison With Window Method Based on FIR.**

| Parameter | Name | Value |
|---|---|---|
| N | Number of Elements | 7 |
| bw | Null to Null Beamwidth | $\leq 120°$ |
| sll | Sidelobe Level | $\leq -52dB$ |
| d | Space between Element | half wavelength |
| $\xi$ | Steering Direction | 0 |

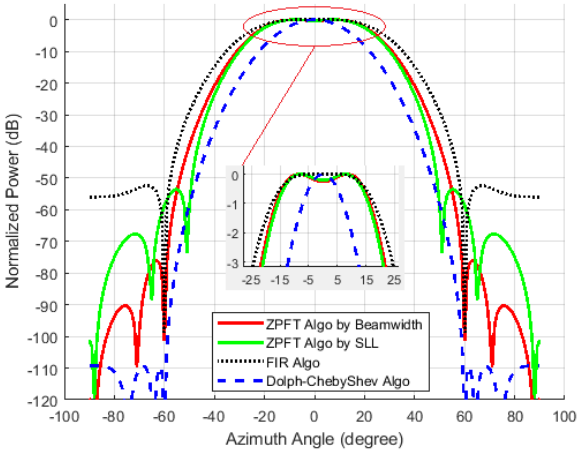


**FIGURE 5. Synthesized beam pattern comparison between FIR, ZPFT and Dolph-ChebyShev.**

main beam width of 25°, the same null to null beamwidth of 60° and a negligible ripple of 0.25dB as shown from the zoomed view of the flat top pattern in Fig. 5. When SLL is a design parameter, the proposed ZPFT algorithm by SLL gives the much narrower null to null beamwidth of 102° with the same SLL level of around -52dB and the same flat-top main beamwidth of 25°. As for the Dolph-Chebyshev algorithm, although it achieves the lowest SLL of around $-110$dB, it has no control of the beam pattern of the main beam.

Table (2) shows the synthesized array using the 3 algorithms where ZPFT is simulated twice with two different controlling parameter. The null to null beamwidth controlled ZPFT is labled as ZPFT-bw while SLL controlled ZPFT is labled as ZPFT-sll.

**TABLE 2. Synthesized ULA for Dolph-Chebyshev, FIR and ZPFT.**

| Weight | Dolph-Chebyshev | FIR | ZPFT-bw | ZPFT-sll |
|---|---|---|---|---|
| 1 | 1 | -0.0345 | 1 | 1 |
| 2 | 5.7194 | 0 | 4.1955 | 3.9514 |
| 3 | 13.8972 | 0.2849 | 6.5144 | 6.1855 |
| 4 | 18.3554 | 0.4992 | 3.7567 | 4.2607 |
| 5 | 13.8972 | 0.2849 | -0.8395 | 0.3377 |
| 6 | 5.7194 | 0 | -1.8773 | -1.1795 |
| 7 | 1 | -0.0345 | -0.6000 | -0.4907 |

For the listed three algorithms, the parameter of the beam width and SLL are interlinked and can't be controlled independently. In the above simulation, the same width of the flat main beam pattern is achieved for both FIR and ZPFT. But as demonstrated, when null to null beamwidth is specified, ZPFT-bw gives much better attenuation in the sidelobe which is around 22dB lower than the FIR algorithm. When the SLL is specified, ZPFT gives a much narrower null to null beamwidth which is around 18° narrower. Although the Dolph-Chebyshev synthesized pattern has the lowest SLL, it is not suitable for the intended usage where flat top beam pattern is needed for robust beamforming to cater for DOA mismatch.

### *B. FASTER CALCULATION SPEED COMPARED WITH NUMERICAL OPTIMIZATION METHOD*

The second simulation is set up to demonstrate that compared with the iteration based global optimisation methods like SDR, the proposed ZPFT can deliver the same optimal beam performance but with much lower computation complexity. The design parameter is listed in Table (3).

**TABLE 3. Design Parameter for Simulation of Comparison With SDR.**

| Parameter | Name | Value |
|---|---|---|
| N | Number of Elements | 8 |
| bw | Null to Null Beamwidth | 106° |
| d | Space between Element | half wavelength |
| $\xi$ | Steering Direction | 0 |
| pr | Passband Ripple | $\leq$ 2dB |

Fig. 6 shows the synthesized beam. The optimization objective is set to minimize the stop band response and the pass band ripple is set to less than 2dB. ZPFT achieves the same pass band performance. Only at the first sidelobe as shown in the zoomed view in Fig. 6, ZPFT shows around 2dB lesser attenuation. But at the far end, it achieves much better attenuation.

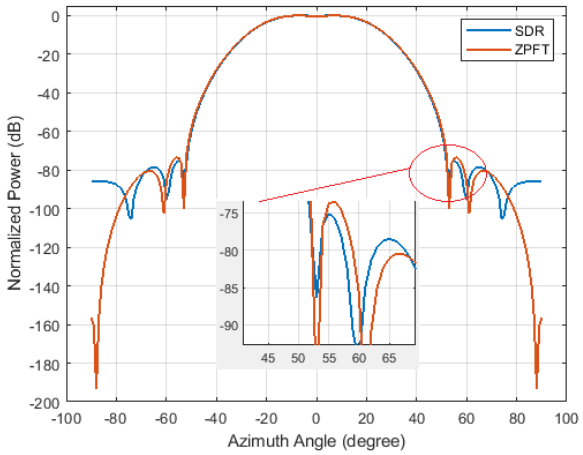


**FIGURE 6. Synthesized beam pattern comparison between SDR and ZPFT.**

Table (4) shows the synthesized array with the two algorithm SDR and ZPFT.

With this comparable performance, ZPFT takes only 0.003 seconds. Compared with 1.15 seconds of the SDR method, ZPFT runs 383 times faster than SDR in an Intel Core i7 Windows laptop where CVX [31] 2.2 software is used

**TABLE 4.** Synthesized ULA for SDR and ZPFT.

| Weight | Semi-definite Relaxation | ZPFT |
|---|---|---|
| 1 | -0.0321730 | 1 |
| 2 | -0.1107191 | 4.94610614 |
| 3 | -0.0667814 | 10.0811574 |
| 4 | 0.27006853 | 10.2004021 |
| 5 | 0.64181062 | 4.14318630 |
| 6 | 0.63031549 | -1.2397797 |
| 7 | 0.30998210 | -1.8366604 |
| 8 | 0.06326148 | -0.5190451 |

for the SDR implementation. This makes it suitable for real time applications as required in high speed rail scenario.

### C. IMPACT OF k FACTOR AND STEERING OF MAIN BEAM BY ANGLE SHIFT

The third simulation is set up to illustrate the effects of shape factor $k$ on the flattened pattern. To verify the impact of the controlling factor, a simulation for 8 elements antenna with different controlling factor $k$ is conducted. The design parameter is listed below in Table (5)

**TABLE 5.** Design Parameter for Impact of Shape Factor $k$ Simulation.

| Parameter | Name | Value |
|---|---|---|
| N | Number of Elements | 8 |
| bw | Null to Null Beamwidth | 100° |
| d | Space between Element | half wavelength |
| $\xi$ | Steering Direction | 0 |
| pr | Passband Ripple | $\leq$ 3dB |

Fig. 7 shows the effect of $k$ on the beam shape. It is clear that the higher the value of $k$, the narrower the beam width. The broadening of the beam width comes with a price of increased SLL. When $k$ decrease from 10 to 0.5, the SLL increased from $-58$dB to $-50$dB. From the zoomed view of the main beam in Fig. 7, it is clear that when $k$ is decreasing from 10 to 0.5, the ripple in the main beam increases from 0 to 3dB.

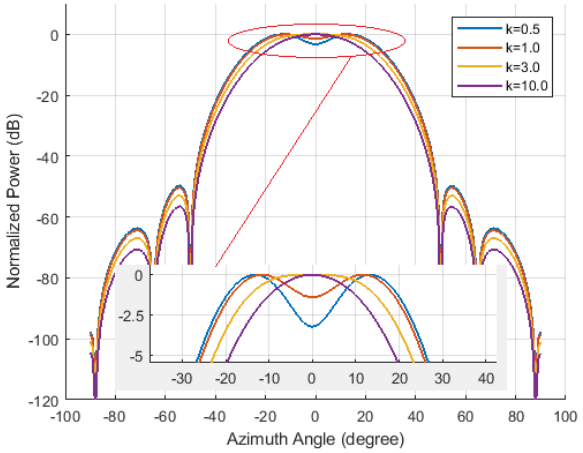


**FIGURE 7.** Beam pattern effect of controlling factor $k$.

Since the ZPFT algorithm is directly working in the spatial angular domain, the steering of the main beam becomes straight forward. It could be implemented by just shifting the angle of the derived zeros. To illustrate the shifting capability, the design parameter is listed below in Table (6)

**TABLE 6.** Design Parameter for Main Beam Shifting Simulation.

| Parameter | Name | Value |
|---|---|---|
| N | Number of Elements | 20 |
| bw | Null to Null Beamwidth | 50° |
| d | Space between Element | half wavelength |
| $\xi$ | Steering Direction | $-15°, 0°, 15°, 20°$ |
| pr | Passband Ripple | $\leq$ 1dB |

Fig. 8 shows the steering of the DOA of the synthesized 20 elements ULA with the above parameter.

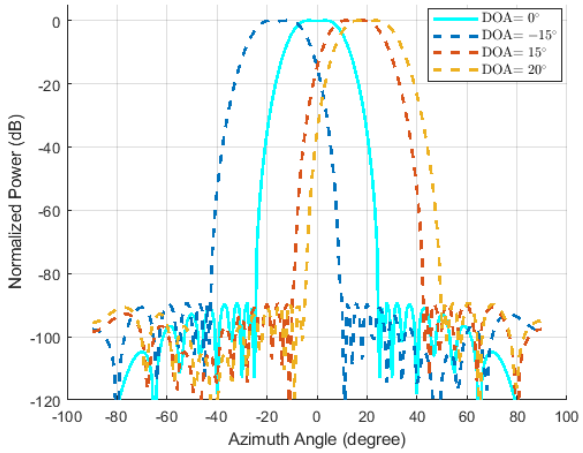


**FIGURE 8.** Main beam steering control for ZPFT algorithm.

In practical scenario, a value of 1-3 would be recommended for $k$ to get a flat top beam pattern with pass band ripple less than 1dB. In this article, $k = 1$ is set for the first simulation, while $k = 2$ is set for the rest of simulations.

## V. CONCLUSION

By breaking the array factor into two separate parts, a flat-top and narrow main beam with low SLL could be synthesized directly in the $Z$ domain. The beam width requirement with low SLL is realized through the use of Dolph-Chebyshev array or other suitable window methods. The flat-top constraint is realized through two reserved zeros in the real axis where one of the zero is derived from the analysis of the broadening effect of two quadratic functions and the other zero is placed for keeping the SLL low. The simulation results confirm that ZPFT can achieve 22dB lower SLL while maintaining the same main beam performance as compared with FIR method for a 7 elements ULA. It can achieve the same optimal performance as demonstrated by the iteration based global optimisation techniques, with about 380 times less computing time in an Intel Core i7 platform. ZPFT can steer the main beam easily in real time by just doing an angle shift

in the unit circle which makes it suitable for high mobility application where the DOA is changing fast.

## REFERENCES

[1] S. Dai, M. Li, Q. H. Abbasi, and M. A. Imran, "A fast blocking matrix generating algorithm for generalized sidelobe canceller beamformer in high speed rail like scenario," *IEEE Sensors J.*, early access, Jun. 15, 2020, doi: 10.1109/JSEN.2020.3002699.

[2] M. Er and A. Cantoni, "Derivative constraints for broad-band element space antenna array processors," *IEEE Trans. Acoust., Speech, Signal Process.*, vol. 31, no. 6, pp. 1378–1393, Dec. 1983.

[3] C.-Y. Chen and P. P. Vaidyanathan, "Quadratically constrained beamforming robust against Direction-of-Arrival mismatch," *IEEE Trans. Signal Process.*, vol. 55, no. 8, pp. 4139–4150, Aug. 2007.

[4] B. Liao, C. Guo, L. Huang, Q. Li, and H. C. So, "Robust adaptive beamforming with precise main beam control," *IEEE Trans. Aerosp. Electron. Syst.*, vol. 53, no. 1, pp. 345–356, Feb. 2017.

[5] Y. Zhang, W. He, W. Hong, and Z. Song, "Flat topped radiation pattern synthesis based on FIR filter concept," in *Proc. IEEE Asia Pacific Microw. Conf. (APMC)*, Nov. 2017, pp. 751–754.

[6] A. Reyna, L. I. Balderas, and M. A. Panduro, "Time-modulated antenna arrays for circularly polarized shaped beam patterns," *IEEE Antennas Wireless Propag. Lett.*, vol. 16, pp. 1537–1540, 2017.

[7] Y. Xu, X. Shi, W. Li, and J. Xu, "Flat-top beampattern synthesis in range and angle domains for frequency diverse array via second-order cone programming," *IEEE Antennas Wireless Propag. Lett.*, vol. 15, pp. 1479–1482, 2016.

[8] A. K. Singh, M. P. Abegaonkar, and S. K. Koul, "Wide angle beam steerable high gain flat top beam antenna using graded index metasurface lens," *IEEE Trans. Antennas Propag.*, vol. 67, no. 10, pp. 6334–6343, Oct. 2019.

[9] J. Wang, Y. Yao, J. Yu, and X. Chen, "Broadband compact smooth horn with flat-top radiation pattern," *Electron. Lett.*, vol. 55, no. 3, pp. 119–120, Feb. 2019.

[10] J. Khalilpour, J. Ranjbar, and P. Karami, "A novel algorithm in a linear phased array system for side lobe and grating lobe level reduction with large element spacing," *Analog Integr. Circuits Signal Process. volume*, vol. 104, pp. 1–11, Mar. 2020.

[11] S. Das, G. R. Hardel, P. Chakravorty, D. Mandal, R. Kar, and D. S. P. Ghoshal, "Optimization of antenna arrays for SLL reduction towards Pareto objectivity using GA variants," in *Proc. IEEE Symp. Ser. Comput. Intell.*, Dec. 2015, pp. 1164–1169.

[12] S. A. Schelkunoff, "A mathematical theory of linear arrays," *Bell Syst. Tech. J.*, vol. 22, no. 1, pp. 80–107, Jan. 1943.

[13] C. L. Dolph, "A current distribution for broadside arrays which optimizes the relationship between beam width and side-lobe level," *Proc. IRE*, vol. 34, no. 6, pp. 335–348, Jun. 1946.

[14] G. B. Arfken, *Mathematical Methods for Physicists*, 6th ed. New York, NY, USA: Academic, Jul. 2005. [Online]. Available: https://www.xarg.org/ref/a/0120598760/

[15] H. Riblet, "Discussion on a current distribution for broadside arrays which optimizes the relationship between beamwidth and side-lobe level," *Proc. Ire*, vol. 35, pp. 489–492, May 1947.

[16] T. T. Taylor, "Design of line-source antennas for narrow beamwidth and low side lobes," *Trans. IRE Prof. Group Antennas Propag.*, vol. 3, no. 1, pp. 16–28, Jan. 1955.

[17] A. Villeneuve, "Taylor patterns for discrete arrays," *IEEE Trans. Antennas Propag.*, vol. AP-32, no. 10, pp. 1089–1093, Oct. 1984.

[18] G. Buttazzoni and R. Vescovo, "Gaussian approach versus dolph-chebyshev synthesis of pencil beams for linear antenna arrays," *Electron. Lett.*, vol. 54, no. 1, pp. 8–10, Jan. 2018.

[19] M. Matijascic and G. Molnar, "Design of linear arrays forming pencil beams based on derivatives of chebyshev polynomials," in *Proc. 42nd Int. Conv. Inf. Commun. Technol., Electron. Microelectron. (MIPRO)*, May 2019, pp. 117–121.

[20] G. T. Freitas de Abreu and R. Kohno, "A modified Dolph-Chebyshev approach for the synthesis of low sidelobe beampatterns with adjustable beamwidth," *IEEE Trans. Antennas Propag.*, vol. 51, no. 10, pp. 3014–3017, Oct. 2003.

[21] M. Okuda, M. Ikehara, and S. Takahashi, "Fast and stable least-squares approach for the design of linear phase FIR filters," *IEEE Trans. Signal Process.*, vol. 46, no. 6, pp. 1485–1493, Jun. 1998.

[22] W. Fan, C. Zhang, and Y. Huang, "Flat beam design for massive MIMO systems via Riemannian optimization," *IEEE Wireless Commun. Lett.*, vol. 8, no. 1, pp. 301–304, Feb. 2019.

[23] D. Mandal, K. S. Kola, J. Tewary, V. P. Roy, and A. K. Bhattacharjee, "Synthesis of steered flat-top beam pattern using evolutionary algorithm," *Adv. Electromagn.*, vol. 5, no. 3, pp. 86–90, 2016.

[24] B. Misra and A. Deb, "Synthesis of antenna arrays with flat-top pattern using conventional and random drift particle swarm optimization algorithms," in *Proc. Emerg. Trends Electron. Devices Comput. Techn. (EDCT)*, Mar. 2018, pp. 1–5.

[25] A. Gershman, N. Sidiropoulos, S. Shahbazpanahi, M. Bengtsson, and B. Ottersten, "Convex optimization-based beamforming," *IEEE Signal Process. Mag.*, vol. 27, no. 3, pp. 62–75, May 2010.

[26] W. Liu and S. Weiss, *Wideband Beamforming: Concepts and Techniques*, vol. 17. Hoboken, NJ, USA: Wiley, 2010.

[27] H. L. Van Trees, *Optimum Array Processing: Part IV of Detection, Estimation, and Modulation Theory*. Hoboken, NJ, USA: Wiley, 2004.

[28] S. J. Orfanidis, "Electromagnetic waves and antennas," Dept. Electron. Commun. Eng., Rutgers Univ., Piscataway, NJ, USA, Tech. Rep., 2002.

[29] R. C. Hansen, "Array pattern control and synthesis," *Proc. IEEE*, vol. 80, no. 1, pp. 141–151, 1992.

[30] A. Boyajian, "Physical interpretation of complex angles and their functions," *J. Amer. Inst. Electr. Engineers*, vol. 42, no. 2, pp. 155–164, Feb. 1923.

[31] M. Grant and S. Boyd. *CVX: MATLAB Software for Disciplined Convex Programming, Version 2.1*. Accessed: Mar. 2014. [Online]. Available:http://cvxr.com/cvx

[32] Z.-Q. Luo, W.-K. Ma, A. So, Y. Ye, and S. Zhang, "Semidefinite relaxation of quadratic optimization problems," *IEEE Signal Process. Mag.*, vol. 27, no. 3, pp. 20–34, May 2010.

[33] X. Zhang, Z. He, X. Zhang, and W. Peng, "High-performance beampattern synthesis via linear fractional semidefinite relaxation and quasi-convex optimization," *IEEE Trans. Antennas Propag.*, vol. 66, no. 7, pp. 3421–3431, Jul. 2018.

[34] B. Fuchs, "Application of convex relaxation to array synthesis problems," *IEEE Trans. Antennas Propag.*, vol. 62, no. 2, pp. 634–640, Feb. 2014.

**SHAOWEI DAI** received the B.Sc. and M.Sc. degrees in electronic engineering from Wuhan University. He is currently pursuing the Ph.D. degree in electronics & electrical engineering with the University of Glasgow. He was a Research Associate with Nanyang Technological University (NTU). He has been a Chief Technology Officer of RFNet Technologies. His research interests include wireless communication, smart antenna, signal processing, and artificial intelligence in both fundamental algorithm research and system development.

**MINGHUI LI** (Member, IEEE) has been a Lecturer with the Centre for Ultrasonic Engineering, Department of Electronic and Electrical Engineering, University of Strathclyde, U.K. He is currently an Associate Professor of electronic systems with the University of Glasgow, based in Singapore (UGS). He has investigated a range of industrial, UK EPSRC, knowledge exchange, and university strategic research projects as a principal investigator or a co-investigator, through collaboration and partnership with industrial companies and R&D organisations like Rolls Royce, Shell, E.ON, Serco, and the National Nuclear Laboratory from key sectors of Energy, Oil and Gas, Aerospace, Nuclear, Transportation and Healthcare in U.K. His research interests include sensing systems, signal processing and imaging in both fundamental algorithm research and applied prototype system development, covering a diversity of applications in communications, radar, sonar, nondestructive evaluation (NDE), and biomedical diagnosis and imaging.

**QAMMER H. ABBASI** (Senior Member, IEEE) received the B.Sc. and M.Sc. degrees (Hons.) in electronics and telecommunication engineering from the University of Engineering and Technology (UET) Lahore, Lahore, Pakistan, and the Ph.D. degree in electronic and electrical engineering from the Queen Mary University of London (QMUL), U.K., in January 2012. From 2012 to June 2012, he was a Postdoctoral Research Assistant with the Antenna and Electromagnetics Group, QMUL. From 2012 to 2013, he was an International Young Scientist under the National Science Foundation China (NSFC) and an Assistant Professor with the University of Engineering and Technology (UET), KSK, Lahore. From August 2013 to April 2017, he was with the Center for Remote healthcare Technology and Wireless Research Group, Department of Electrical and Computer Engineering, Texas A &M University (TAMUQ) initially as an Assistant Research Scientist and later was promoted to an Associate Research Scientist and a Visiting Lecturer, where he was leading multiple Qatar national research foundation grants. He is currently a Senior Lecturer (Associate Professor) with the James Watt School of Engineering, University of Glasgow, in addition to a Visiting Lecturer with the Queen Mary, University of London (QMUL). He has been mentoring several undergraduate, graduate students, and postdocs. He has research portfolio of around £5 million and contributed to ten books and more than 300 leading international technical journal and peer reviewed conference papers and received several recognitions for his research. He contributed in organizing several IEEE conferences, workshop, and special sessions in addition to European school of antenna course. His research interests include antennas, bio-electromagnetics, nano communication, Terahertz sensing, the Internet of Things, biomedical applications of millimeter and terahertz communication, wearable and flexible sensors, antenna interaction with human body, implants, body centric wireless communication issues, wireless body sensor networks, noninvasive health care solutions, and physical layer security for wearable/implant communication.

Dr. Abbasi is a member of IET and a Commitee Member of IET Antenna & Propagation and Healthcare Network. He has been a member of the technical program committees of several IEEE flagship conferences and a technical reviewer for several IEEE and top notch journals, including a TPC chair of 4th International UCET Conference 2019 and an Executive Chair of the 5th International UCET Conference 2020. He received several recognitions for his research, which includes appearance in BBC, STV, dawnnews, local, and international newspaper, cover of MDPI journal, most downloaded articles, U.K. exceptional talent endorsement by the Royal academy of Engineering, the National Talent Pool Award by Pakistan, the International Young Scientist Award by NSFC China, the URSI Young Scientist Award, National interest waiver by USA, six best paper awards, and best representative image of an outcome by QNRF. He is a Chair of the IEEE AP/MTT Scotland Chapter, the IEEE AP Young Professional Committee Member, and a Chair of the IEEE Young Professional Affinity Group. He is an Associate Editor of the IEEE JOURNAL OF ELECTROMAGNETICS, RF, AND MICROWAVES IN MEDICINE AND BIOLOGY, the IEEE SENSORS, the IEEE OPEN ACCESS ANTENNA AND PROPAGATION, and IEEE ACCESS journal. He is acting as a guest editor for numerous special issues in top notch journals.

**MUHAMMAD ALI IMRAN** (Senior Member, IEEE) received the M.Sc. (Hons.) and Ph.D. degrees from Imperial College London, U.K., in 2002 and 2007, respectively. From June 2007 to August 2016, he was with the 5G Innovation Centre, University of Surrey, U.K., where he is also a Visiting Professor. He is currently a Professor of communication systems with the University of Glasgow, also the Dean of the University of Glasgow UESTC, also the Head of Communications Sensing and Imaging (CSI) Research Group, and also the Director of the Glasgow UESTC Centre of Educational Development and Innovation. He is also an affiliate Professor of The University of Oklahoma, USA. He has led a number of multimillion-funded international research projects encompassing the areas of energy efficiency, fundamental performance limits, sensor networks, and self-organizing cellular networks. He also led the new physical layer work area for 5G Innovation Centre, Surrey. He has a global collaborative research network spanning both academia and key industrial players in the field of wireless communications. He has supervised more than 40 successful Ph.D. graduates and published more than 400 peer-reviewed research articles, including more than 50 IEEE Transaction articles.

Dr. Imran is a Fellow of IET and a Senior Fellow of the Higher Education Academy (SFHEA), U.K. He has been awarded the IEEE Comsoc's Fred Ellersick Award 2014, TAO's Best Paper Award in IEEE ICC 2019, FEPS Learning and Teaching Award 2014, the Sentinel of Science Award 2016, and the twice nominated for Tony Jean's Inspirational Teaching Award. He received more than seven best paper awards in international conferences. He is a shortlisted finalist for The Wharton-QS Stars Awards 2014 for Innovative Teaching and VC's Learning and Teaching Award in the University of Surrey. He secured first rank in his B.Sc. and in his M.Sc. degree (Hons.) along with an award of excellence in recognition of his academic achievements conferred by the President of Pakistan. He is the UK&RI Chair of the Backhaul/Fronthaul Networking & Communications Emerging Technologies Initiatives (ETI-BNC), IEEE ComSoc. He has been an Associate Editor of the IEEE COMMUNICATIONS LETTERS and *IET Communications Journal*. He is currently serving as an Associate Editor for the IEEE TRANSACTIONS ON COMMUNICATIONS and IEEE ACCESS. He has served as guest editor for many prestigious international journals including the IEEE JOURNAL ON SELECTED AREAS IN COMMUNICATIONS (JSAC). He has given an invited TEDx talk (2015) and more than 50 plenary talks, tutorials, and seminars in international conferences, events and other institutions. He has taught on international short courses in USA and China. He is the Co-Founder of the IEEE Workshop BackNets 2015 and chaired several tracks/workshops of international conferences.